

研究成果の刊行に関する一覧表

書籍

著者氏名	論文タイトル名	書籍全体の編集者名	書籍名	出版社名	出版地	出版年	ページ
脇口 宏	小児の無菌性髄膜炎.	山口徹, 北原光夫, 横井次矢	今日の治療指針2009	医学書院	東京	2009	1039
脇口 宏	第10章.感染症, 寄生虫疾患. 細菌感染症 B.1.髄膜炎菌感染症, D.6.百日咳, ウイルス感染症7. 突発性発疹, 8. 急性灰白髄炎, 9. コクサッキーウイルス・エコー(ECHO)ウイルス感染症	高久文麿, 尾形悦郎, 黒川清, 矢崎義雄	新臨床内科学(第9版)	医学書院	東京	2009	1308-10, 1327-8, 1357-8, 1359-60
脇口 宏, 藤枝幹也	Ⅲ感染症など 31. インフルエンザ, 32. 麻疹, 33. 風疹.	五十嵐隆	目で見ると小児救急	文光堂	東京	2009	132-137
脇口 宏	成人の百日咳.	砂川慶介, 森島恒雄, 堤裕幸, 津村直幹	こどもの感染症のみかた	臨床医薬研究会	東京	2009	123-124
脇口 宏	第14章 感染症 A 総論, B ウイルス感染症, C クラミジア感染症, D リケッチャ感染症.	森川昭廣	標準小児科学	医学書院	東京	2009	324-353
脇口 宏	第15章 呼吸器疾患 E上気道疾患, F下気道疾患. 標準小児科学	森川昭廣	標準小児科学	医学書院	東京	2009	386-404

雑誌

発表者氏名	論文タイトル名	発表誌名	巻号	ページ	出版年
Imadome K, Shimizu N, Yajima M, Watanabe K, Nakamura H, Takeuchi H, and Fujiwara S.	CD40 signaling activated by Epstein-Barr virus promotes cell survival and proliferation in gastric carcinoma-derived human epithelial cells.	Microbes and Infection	11	429-433	2009
Inomata H, Takei M, Nakamura H, Fujiwara S, Shiraiwa. H., Kitamura N, Hirohata S, Masuda H, Takeuchi J, and Sawada S.	Epstein-Barr-Virus-Infected CD15 (Lewis X)-Positive Hodgkin-Lymphoma-like B Cells in Patients with Rheumatoid Arthritis.	Open Rheumatol J.	3	41-47	2009
Miyagawa, Y., Kiyokawa N., Ochiai, N., Imadome, K., Horiuchi, Y., Onda K., Yajima, M., Nakamura, H., Katagiri, U., Okita H., Morio, T., Shimizu, N., Fujimoto, J., and Fujiwara, S	Ex vivo expanded cord blood CD4 T lymphocytes exhibit distinct expression profile of cytokine-related genes from those of peripheral blood origin.	Immunology	128	405-419	2009
Yajima, M., Imadome, K., Nakagawa, A., Watanabe, S., Terashima, K., Nakamura, H., Ito, M., Shimizu, N., Yamamoto, N., and Fujiwara, S.	T-cell-mediated control of Epstein-Barr virus infection in humanized mice.	J Infect Dis.	200	1611 - 1615	2009
Arai, A., Imadome, K., Fujiwara, S. and Miiura O.	Autoimmune hemolytic anemia accompanied by reactivation of an Epstein-Barr virus infection with suppressed CTL response to EBV-infected cells in an elderly man.	Inter. Med.,		in press	
Wakabayashi, S.Arai, A., Oshikawa, G., Arai, A., Watanabe, M., Uchida, N., Taniguchi, S., Miiura, O	Extranodal NK/T cell lymphoma, nasal type, of the small intestine diagnosed by double-balloon endoscopy.	Int J Hematol	90	605-610	2009
Kimura H, Miyake K, Yamauchi Y, Nishiyama K, Iwata S, Iwatsuki K, Gotoh K, Kojima S, Ito Y, Nishiyama Y.	Identification of Epstein-Barr virus (EBV)-infected lymphocyte subtypes by flow cytometric in situ hybridization in EBV-associated lymphoproliferative diseases.	J Infect Dis	200	1078-1087	2009
Nagasawa M., Ogawa K., Nagata K., Shimizu N.	Serum granulysin as a possible biomarker of NK cell neoplasm.	J Haematol		[Epub ahead of print]	2009 Nov 13

Yajima M, Imadome KI, Nakagawa A, Watanabe S, Terashima K, Nakamura H, Ito M, Shimizu N, Yamamoto N, Fujiwara S.T	T cell-Mediated Control of Epstein-Barr Virus Infection in Humanized Mice.	<i>J Infect Dis.</i>		1611-1615	2009 Nov 15
Iwata S, Wada K, Tobita S, Gotoh K, Ito Y, Demachi-Okamura A, Shimizu N, Nishiyama Y, Kimura H.	Quantitative Analysis of Epstein-Barr Virus (EBV)-Related Gene Expression in Patients with Chronic Active EBV Infection.	<i>J Gen Virol.</i>		[Epub ahead of print]	2009 Sep 30
Yamanaka Y., Tagawa H., Takahashi N., Watanabe A., Guo Y-M., Iwamoto K., Yamashita J., Saitoh H., Kameoka Y., Shimizu N., Ichinohasama R., and Sawada K.	Aberrant overexpression of microRNAs activate AKT signaling via down-regulation of tumor suppressors in natural killer-cell lymphoma/ leukemia.	<i>Blood</i>	114	3265-3275	2009
Moriai S, Takahara M, Ogino T, Nagato T, Kishibe K, Ishii H, Katayama A, Shimizu N and Harabuchi Y.	Production of Interferon- γ -Inducible Protein-10 and Its Role as an Autocrine Invasion Factor in Nasal Natural Killer/T-Cell Lymphoma Cells.	<i>Clin Cancer Res.</i>	15(22)	6771-6779	2009
Miyagawa Y., Kiyokawa N., Ochiai N., Imadome K., Horiuchi Y., Onoda K., Yajima M., Nakamura H., Katagiri Y., Okita H., Morio T., Shimizu N., Fujimoto J. and Fujiwara S.	Ex vivo expanded cord blood CD4 T lymphocytes exhibit a distinct expression profile of cytokine-related genes from those of peripheral blood origin.	<i>Immunology</i>	128	405-419	2009
Imadome K, Shimizu N, Yajima M, Watanabe K, Nakamura H, Takeuchi H, Fujiwara S.	CD40 signaling activated by Epstein-Barr virus promotes cell survival and proliferation in gastric carcinoma-derived human epithelial cells.	<i>Microbes Infect</i>	11(3)	429-433	2009
Ono Y., Terashima K., Liu A., Yokoyama M., Yokoshima K., Mizukami M., Watanabe K., Mochimaru Y., Furusaka T., Shimizu N., Yamamoto N., Ishiwata T., Sugisaki Y., Yagi T. and Naito Z.	Follicular dendritic cell sarcoma with microtubuloreticular structure and virus-like particle production <i>in vitro</i> .	<i>Pathol.Int.</i>	59	332-344	2009

Albert MH, Bittner TC, Nonoyama S, Notarangelo LD, Burns S, Imai K, Espanol T, Fasth A, Pellier I, Strauss G, Morio T , Gathmann B, Noordzij JG, Fillat C, Hoenig M, Nathrath M, Meindl A, Pagel P, Wintergerst U, Fischer A, Thrasher AJ, Belohradsky BH, Ochs HD.	X-linked thrombocytopenia (XLT) due to WAS mutations: Clinical characteristics, long-term outcome, and treatment options.	<i>Blood</i> .	[Epub ahead of print]		2010, Feb, 19.
Oba D, Hayashi M, Minamitani M, Hamano S, Hisaka N, Kikuchi A, Kishimoto H, Takagi M, Morio T , Mizutani S.	Autopsy study of cerebellar degeneration in siblings with ataxia-telangiectasia-like disorder (ATLD)	<i>Acta Neuroathologica</i> .	(in press).		2010
Inoue H, Takada H, Kusuda T, Goto T, Ochiai M, Kinjo T, Muneuchi J, Takahata Y, Takahashi N, Morio T , Kosaki K, Hara T.	Successful cord blood transplantation for a CHARGE syndrome with CHD7 mutation showing DiGeorge sequence including hypoparathyroidism.	<i>Eur J Pediatr</i> .	[Epub ahead of print]		2010
Nanki T, Takada K, Komano Y, Morio T , Kanegane H, Nakajima A, Lipsky PE, Miyasaka N.	Chemokine receptor expression and functional effects of chemokines on B cells: implication in the pathogenesis of rheumatoid arthritis.	<i>Arthritis Res Ther</i> .	11(5)	R149. [Epub ahead of print]	2009
Miyanaga M, Sugita S, Shimizu N, Morio T , Miyata K, Mochizuki M.	A significant association of viral loads with corneal endothelial cell damage in cytomegalovirus anterior uveitis.	<i>Br J Ophthalmol</i> .	[Epub ahead of print]		2009 Sep 3.
Hasegawa D, Kaji M, Takeda H, Kawasaki K, Takahashi H, Ochiai H, Morio T , Omori Y, Yokozaki H, Kosaka Y.	Fatal degeneration of specialized cardiac muscle associated with chronic active Epstein-Barr virus infection.	<i>Pediatr Int</i> .	51	846-8	2009
Miyagawa Y, Kiyokawa N, Ochiai N, Imadome K-I, Horiuchi Y, Onda K, Yajima M, Nakamura H, Katagiri YU, Okita H, Morio T , Shimizu N, Fujimoto J, Fujiwara S.	<i>Ex vivo</i> expanded cord blood CD4 T lymphocytes exhibit a distinct expression profile of cytokine-related genes from those of peripheral blood origin.	<i>Immunology</i>	128	405-419	2009

Morinishi Y, Imai K, Nakagawa N, Sato H, Horiuchi K, Ohtsuka Y, Kaneda Y, Taga T, Hisakawa H, Miyaji R, Endo M, Oh-Ishi T, Kamachi Y, Akahane K, Kobayashi C, Tsuchida M, Morio T , Sasahara Y, Kumaki S, Ishigaki K, Yoshida M, Urabe T, Kobayashi	Identification of severe combined immunodeficiency by T-cell receptor excision circles quantification using neonatal Guthrie cards.	J. Pediatr.	155	829-33	2009
Morio T , Takahashi N, Watanabe F, Honda F, Sato M, Takagi M, Imadome KI, Miyawaki T, Delia D, Nakamura K, Gatti RA, Mizutani S.	Phenotypic variations between affected siblings with ataxia-telangiectasia: ataxia-telangiectasia in Japan.	Int.J.Hematol.	90	455-462	2009
Isoda T, Ford A, Tomizawa D, van Delft F, De Castro DG, Mitsui N, Score J, Taki T, Takagi M, Morio T , Saji H, Greaves M, Mizutani S.	Immunologically silent cancer clone transmission from mother to offspring.	Proc.Natl.Acad. Sci. USA.	106	17882-5.	2009
Uchisaka N. Takahashi N. Sato M. Kikuchi A. Mochizuki S. Imai K. Nonoyama S. Ohara O. Watanabe F. Mizutani S. Hanada R. Morio T .	Two brothers with ataxia-telangiectasia-like disorder with lung adenocarcinoma.	J. Pediatr.	155:	435-438,	2009
Futagami Y, Sugita S, Fujimaki T, Yokoyama T, Morio T , Mochizuki M.	Bilateral anterior granulomatous keratouveitis with sunset glow fundus in a patient with autoimmune polyglandular syndrome.	Ocul Immunol Inflamm.	17	88-90,	2009
Takahashi N. Matsukoto K. Saito H. Nanki T. Miyasaka N. Kobata T. Azuma M. Lee S-K. Mizutani S. Morio T .	Impaired CD4 and CD8 effector function and decreased memory T-cell populations in ICOS deficient patients.	Immunol.	182	5515-5527,	2009
Yoshida H. Kusuki S. Hashii Y. Ohta H. Morio T . Ozono K.	Ex vivo-expanded donor CD4 T lymphocyte infusion against relapsing neuroblastoma: A transient Graft-versus-Tumor effect.	Pediatr Blood Cancer	52	895-897,	2009
脇口宏	小児の発疹の診かた。EBウイルス感染症。	小児内科	42	180-184	2010

前田明彦, 藤枝幹也, 脇口 宏	感染後疲労症候群. 小児の症候群.	小児科診療	72	422	2009
前田明彦, 藤枝幹也, 脇口 宏	世界標準にはるかに及ばないわが国の予防接種体制-水痘ワクチンの2回接種の必要性.	日本医師会雑誌	138	694-696	2009
玉城涉, 前田明彦、・・・、脇口 宏	妊婦健診で母の梅毒血清反応が陰性であった先天梅毒の1例	小児感染免疫	21	357-362	2009
久川浩章, 脇口 宏	小児における抗菌薬の適正使用.	臨床と研究	86	487-491	2009
有瀬和美, 武内世生, 竹内啓晃, 前田明彦, 脇口 宏, 倉本 秋	高知大学医学部および附属病院で発生した百日咳アウトブレイク.	感染制御 JICP	5	175-179	2009
佐藤哲也, 前田明彦, 藤枝幹也, 脇口 宏	特集:小児の治療指針「EBウイルス感染症」	小児科診療増刊号	(73巻増刊号)	(印刷中)	
脇口 宏	小児感染症のすべて. □ 感染症の原因微生物別に小児感染症を考える. 13. サイトメガロウイルス, EBウイルス.	化学療法の領域	25(増)	1095-1104	2009
Usui D, Yamaguchi-Shima N, Okada S, Shimizu T, Wakiguchi H, Yokotani K	Central bombesin activates adrenal adrenaline- and noradrenaline- containing cells via brain thromboxane A2 in rats.	Auton Neurosci	147	33-37	2009
Usui D, Yamaguchi-Shima N, Okada S, Shimizu T, Wakiguchi H, Yokotani K	Selective activation of the sympathetic ganglia by centrally administered corticotrophin-releasing factor in rats.	Auton Neurosci	146	111-114	2009
Matsusita K, Uchiyama J, kato S, Ujihara T, Hoshiba H, Sugihara S, Muraoka A, Wakiguchi H, Matsuzaki S	Morphological and genetic analysis of the threebacteriophages of Serratia marcescens isolated from environmental water.	FEMS Micribiol Letters	291	201-208	2009
Shinji T, Kagaya S, Shinohara M, Wakiguchi H, Matsumoto T, Takahata Y, Morimatsu F, Saito H, Matsumoto K	Lactobacillus rhamonosus GG and lactobacillus casei suppress Escherichia coli-induced chemokine expression in intestinal epithelial cells.	Int Arch Allergy Immunol	148	45-58	2009

Uchiyama J, Rashel M, Matsumoto T, Sumiyama Y, Wakiguchi H, matsuzaki S	Characteristics of a novel Pseudomonas aeruginosa bacteriophage, PAJU2, which is generally related to bacteriophage D3.	Virus Res	139	131-134	2009
Uchiyama J, Maeda Y, Takemura I, Chess-Williams R, Wakiguchi H, Matsuzaki S	Blood kinetics of four intraperitoneally-administered therapeutic candidate bacteriophages in healthy and neutropenic mice.	Microbiol Immunol	153	301-304	2009

Identification of Epstein-Barr Virus (EBV)-Infected Lymphocyte Subtypes by Flow Cytometric In Situ Hybridization in EBV-Associated Lymphoproliferative Diseases

Hiroshi Kimura,¹ Kanae Miyake,¹ Yohei Yamauchi,¹ Kana Nishiyama,¹ Seiko Iwata,¹ Keiji Iwatsuki,³ Kensei Gotoh,² Seiji Kojima,² Yoshinori Ito,² and Yukihiko Nishiyama¹

Departments of ¹Virology and ²Pediatrics, Nagoya University Graduate School of Medicine, Nagoya; ³Department of Dermatology, Okayama University Graduate School of Medicine, Dentistry and Pharmaceutical Sciences, Okayama, Japan

To diagnose Epstein-Barr virus (EBV)-associated diseases and to explore the pathogenesis of EBV infection, not only must the EBV load be measured, but EBV-infected cells must also be identified. We established a novel flow cytometric in situ hybridization assay to detect EBV⁺ suspension cells using a peptide nucleic acid probe specific for EBV-encoded small RNA (EBER). By enhancing fluorescence and photostability, we successfully stained EBER and surface antigens on the same cells. In 3 patients with hydroa vacciniforme-like lymphoproliferative disease, we demonstrated that 1.7%–25.9% of peripheral lymphocytes were infected with EBV and specifically identified these lymphocytes as CD3⁺CD4⁻CD8⁻ $\gamma\delta$ T cell receptor-positive T cells. The results indicate that this novel and noninvasive assay is a direct and reliable method of characterizing EBV-infected lymphocytes that can be used not only to diagnose EBV infection but also to clarify the pathogenesis of EBV-associated diseases.

Epstein-Barr virus (EBV) is a ubiquitous virus and occasionally causes infectious mononucleosis in primary infection. In rare cases, chronic active EBV infection develops in apparently immunocompetent hosts [1–3]. EBV preferentially infects B cells through CD21 and HLA class II molecules and establishes latent infection in memory B cells [4]. Several types of B cell-origin lymphomas or lymphoproliferative diseases, including Burkitt lymphoma, Hodgkin lymphoma, primary central nervous system lymphoma, and opportunistic B cell lymphoproliferative disorders, are etiologi-

cally linked to EBV infection [2, 3, 5]. EBV also infects T cells and natural killer (NK) cells and is associated with T/NK lymphoproliferative diseases and lymphoma or leukemia, such as EBV-related hemophagocytic lymphohistiocytosis, systemic EBV⁺ T cell lymphoproliferative disease of childhood, hydroa vacciniforme-like lymphoma, nasal NK cell lymphoma, and aggressive NK cell leukemia [2, 3, 5, 6].

Because EBV is a ubiquitous virus that latently infects various lymphocytes, simply detecting EBV is insufficient to diagnose EBV-associated diseases [7]. To diagnose EBV-associated diseases and to explore the pathogenesis of EBV infection, one must not only measure the EBV load, but one must also identify EBV-infected cells. In situ hybridization (ISH) with the EBV-encoded small RNA (EBER) is widely used to detect EBV-infected cells in tissue specimens [8, 9]. EBER is a good marker for EBV infection because it is detectable in virtually all EBV-infected cells and is expressed at very high levels, reaching 10⁷ molecules per cell [5]. Therefore, EBER ISH is a specific and direct method of identifying EBV-infected cells in tissue specimens [9]. How-

Received 3 March 2009; accepted 6 May 2009; electronically published 21 August 2009.

Potential conflicts of interest: none reported.

Financial support: Ministry of Education, Culture, Sports, Science and Technology, Japan (grant 19591247).

Reprints or correspondence: Dr Kimura, Dept of Virology, Nagoya University Graduate School of Medicine, 65 Tsurumai-cho, Showa-ku, Nagoya 466-8550, Japan (hkimura@med.nagoya-u.ac.jp).

The Journal of Infectious Diseases 2009;200:1078–87

© 2009 by the Infectious Diseases Society of America. All rights reserved.

0022-1899/2009/20007-0010\$15.00

DOI: 10.1086/605610

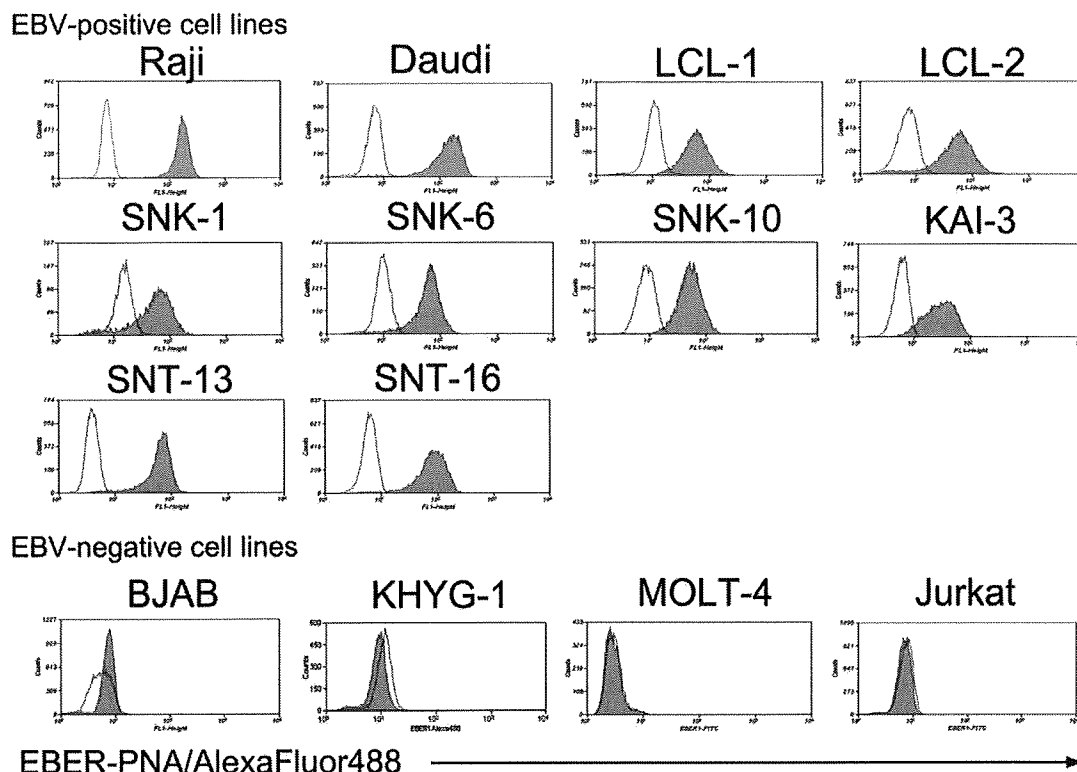


Figure 1. Detection of Epstein-Barr virus (EBV)-encoded small RNA (EBER) by flow cytometric in situ hybridization assay. EBV⁺ or EBV⁻ cells were fixed, permeabilized, and hybridized with either the EBER peptide nucleic acid (PNA) probe (*shaded histograms*) or the negative control PNA probe (*open histograms*). After enhancement of fluorescent signals with Alexa Fluor 488-labeled antibodies, cells were analyzed by flow cytometry. Cell lines included the EBV⁺ B cell lines, Raji, Daudi, lymphoblastoid cell line (LCL) 1, and LCL-2; EBV⁺ natural killer (NK) cell lines, SNK-1, SNK-6, SNK-10, and KAI3; EBV⁺ T cell lines, SNT-13 and SNT-16; EBV⁻ B cell line, BJAB; EBV⁻ NK cell line, KHYG-1; EBV⁻ T cell lines, MOLT-4 and Jurkat. FITC, fluorescein isothiocyanate.

ever, biopsies are invasive and cannot always be performed, owing to the lack of nodal sites or difficulty of access. Because EBV-infected lymphocytes migrate in the peripheral blood in most EBV-associated lymphomas or lymphoproliferative diseases, peripheral blood lymphocytes can be examined instead of tissue specimens [7]. For this reason, applying EBER ISH to peripheral blood would allow EBV-infected cells to be identified and quantified using a more convenient and less invasive procedure.

Peptide nucleic acid (PNA) is a DNA/RNA analog capable of binding to DNA and RNA in a sequence-specific manner [10]. In PNA, nucleobases are attached to a backbone that consists of repetitive units of N-(2-aminoethyl)glycine, in contrast to the sugar-phosphate backbone of DNA/RNA. Because of the high binding affinity of PNA to DNA/RNA and its stability [11, 12], PNA probes have been used for fluorescent ISH to determine telomere lengths at chromosome ends [13–15].

In this study, we established a novel ISH method to detect EBER⁺ suspension cells with flow cytometry using a commercially available EBER PNA probe [16]. By enhancing fluorescence and photostability and modifying the fixation and hy-

bridization steps, we successfully stained both EBER and surface antigens. With this novel flow cytometric ISH (FISH) method, we showed that EBV⁺ $\gamma\delta$ T cells were present in the peripheral blood of patients with hydroa vacciniforme-like lymphoproliferative disease [17], which was defined as an EBV⁺ cutaneous T cell lymphoproliferative disease that occurs in children [6, 18].

METHODS

Cell lines. The EBV⁺ B cell lines included Raji and Daudi, both of which were derived from Burkitt's lymphoma tissue, and 2 lymphoblastoid cell lines transformed with B95-8 EBV. BJAB, an EBV⁻ B cell line, was used as a negative control. The EBV⁺ T cell lines included SNT-13 and SNT-16 [19], and the EBV⁺ NK cell lines included SNK-1, -6, and -10 [19], and KAI3 [20]. These T and NK cell lines were derived either from patients with chronic active EBV infection or from T or NK cell lymphomas. MOLT-4 and Jurkat were used as EBV⁻ T cell lines [21], and KHYG-1 was used as an EBV⁻ NK cell line [22].

Patients and samples. Three patients with hydroa vaccini-

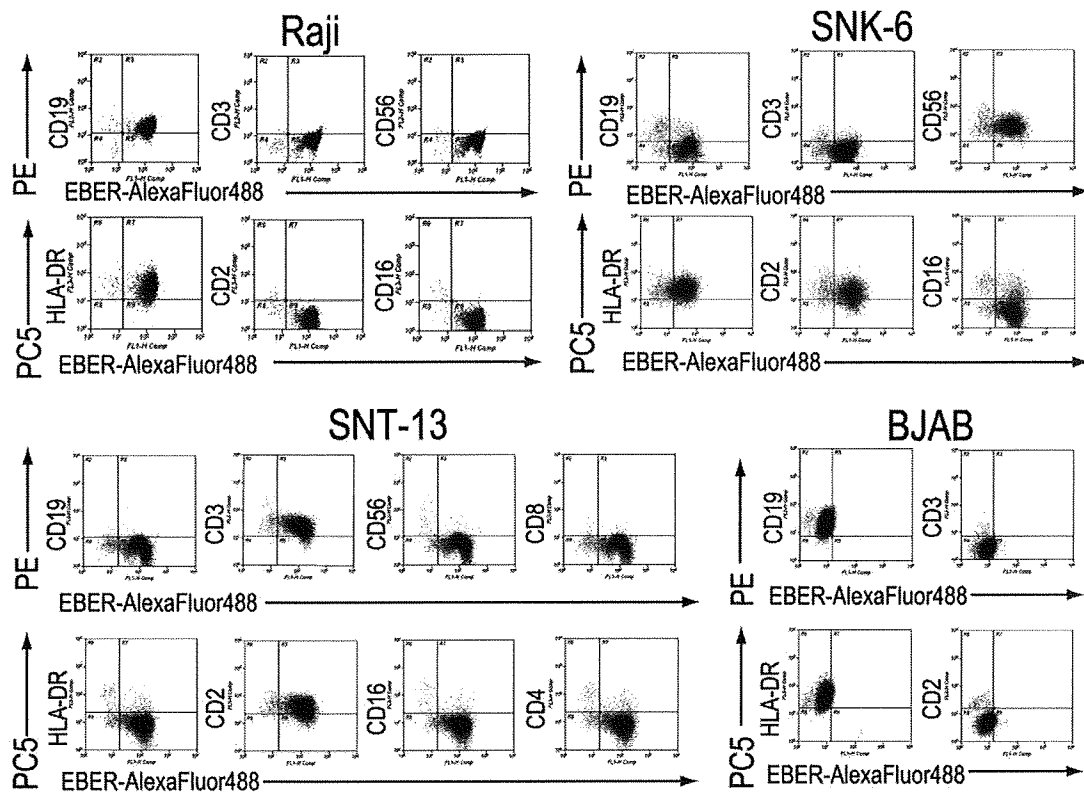


Figure 2. Dual staining for surface antigens and Epstein-Barr virus (EBV)-encoded small RNA (EBER) by flow cytometric in situ hybridization assay. Cells were stained for surface antigens with phycoerythrin (PE)- or PE-cyanin 5 (PC5)-labeled monoclonal antibodies and then fixed, permeabilized, and hybridized with the EBER peptide nucleic acid probe. After enhancement of fluorescent signals, cells were analyzed by flow cytometry. The EBV⁺ B cell line was Raji; the EBV⁺ natural killer (NK) cell line, SNK-6; the EBV⁺ T cell line, SNT-13; and the EBV⁻ B cell line, BJAB.

forme-like lymphoproliferative disease and 1 patient with post-transplantation lymphoproliferative disease were enrolled in the study. As negative controls, 5 healthy volunteers who were seropositive for EBV were also enrolled. Heparinized blood samples were obtained, and peripheral blood mononuclear cells (PBMCs) were separated by density gradients. PBMCs were cryopreserved at -80°C until analysis.

Informed consent was obtained from all patients or guardians and healthy carrier donors. The institutional review board of Nagoya University Hospital approved the use of all specimens examined in this study.

Surface marker staining. Cells were stained with phycoerythrin (PE)-labeled anti-CD3 (clone UCHT1; eBioscience), anti-CD8 (clone B9.11; Immunotech), anti-CD19 (clone HD37; Dako), and anti-CD56 (clone N901; Immunotech) monoclonal antibodies and PE-cyanin 5 (PC5)-labeled anti-CD2 (clone 39C1.5; Immunotech), anti-CD4 (clone 13B8.2; Immunotech), anti-CD16 (clone 3G8; Immunotech), anti-CD56 (clone N901; Immunotech), anti-HLA-DR (clone IMMU357; Immunotech), anti- $\alpha\beta$ T cell receptor (TCR) (clone IP26; eBioscience), and anti-TCR $\gamma\delta$ (clone IMMU510; Immunotech) monoclonal antibodies for 1 h at 4°C . Isotype-matched monoclonal mouse

immunoglobulin (Ig) G antibodies were used in each experiment as controls.

PNA probes. The EBER PNA probe, Y5200, was purchased from Dako. The Y5200 probe is a mixture of 4 different fluorescein-labeled PNA probes complementary to EBER [16]. The negative control PNA probe (Dako), which consists of fluorescein-conjugated random PNA probes, was used as a negative control. The positive control PNA probe (Dako) directed against glyceraldehyde 3-phosphate dehydrogenase was used as a positive control. Each PNA probe was labeled with fluorescein isothiocyanate (FITC).

FISH technique. The following experiments were performed in 1.5-mL microcentrifuge tubes (Corning). For surface marker staining, cells were stained with the appropriate antibodies before fixation and hybridization. Cultured cells (2×10^5) or PBMCs (5×10^5) were fixed with 1% (vol/vol) acetic acid in 4% paraformaldehyde/phosphate buffered saline (PBS) for 40 min at 4°C . After being washed once with PBS, cells were permeabilized in 50 μL of 0.5% Tween 20/PBS at room temperature. Formamide, buffer, and water were added to the cells in permeabilization buffer so that the final formamide and buffer concentrations were the same as the hy-

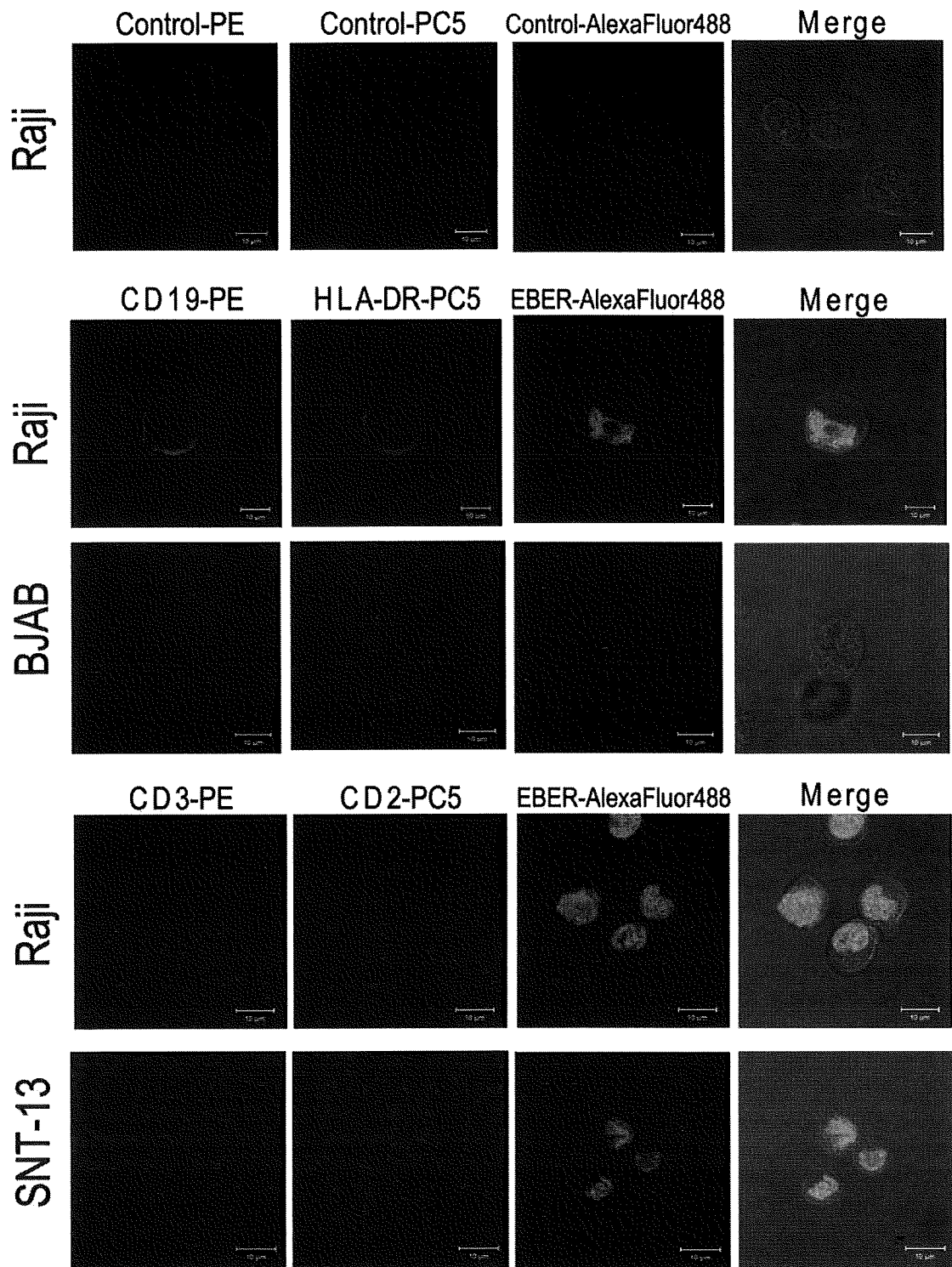


Figure 3. Detection of dual staining for surface antigens and Epstein-Barr virus (EBV)-encoded small RNA (EBER) by confocal microscopy. Cells were stained for surface antigens with phycoerythrin (PE)- or PE-cyanin 5 (PC5)-labeled monoclonal antibodies and then fixed, permeabilized, and hybridized with the EBER peptide nucleic acid probe. After enhancement of fluorescent signals, cells were mounted on glass slides and analyzed by confocal immunofluorescence microscopy. The EBV⁺ B cell line was Raji; the EBV⁻ B cell line, BJAB; and the EBV⁺ T cell line, SNT-13. Bars, 10 μm.

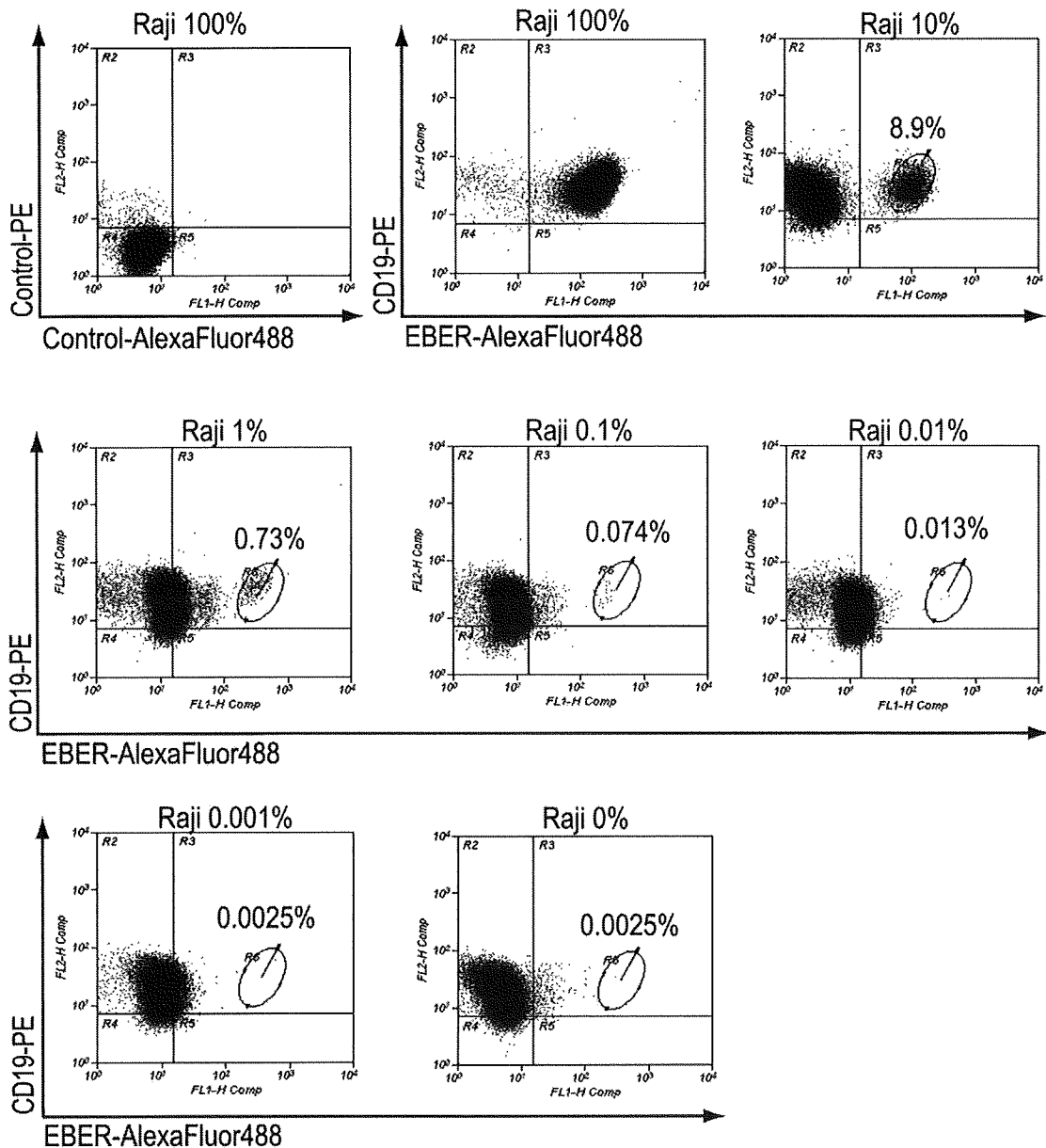


Figure 4. Minimum detection level of cells positive for Epstein-Barr virus (EBV) by flow cytometric in situ hybridization assay. EBV⁺ Raji cells and EBV⁻ BJAB cells were mixed at various ratios, stained with phycoerythrin (PE)-labeled anti-CD19 antibody, and then fixed, permeabilized, and hybridized with the EBV-encoded small RNA (EBER) peptide nucleic acid (PNA) probe. After enhancement of fluorescent signals, the cells were analyzed by flow cytometry. The ratio of Raji to BJAB cells is shown above each quadrant. Numbers in quadrants indicate percentages of CD19⁺EBER⁺ cells.

bridization solution (6% [wt/vol] dextran sulfate, 10 mmol/L sodium chloride, 17.5% [vol/vol] formamide, 0.061% [wt/vol] sodium pyrophosphate, 0.12% [wt/vol] polyvinylpyrrolidone, 0.12% [wt/vol] Ficoll, 5 mmol/L disodium ethylenediaminetetraacetic acid, 50 mmol/L tris(hydroxymethyl) aminomethane [pH 7.5]). The cells were resuspended in 45 μ L of hybridization solution containing 12 nmol/L of the EBER PNA probe, negative control PNA probe, or positive control PNA probe, all FITC labeled. Hybridization was carried out for 1 h at 56°C.

Then cells were washed twice (for 10 and 30 min) with 0.5% Tween 20/PBS at 56°C. To enhance fluorescence and photostability, the Alexa Fluor 488 Signal Amplification Kit (Molecular Probes) was used. The kit protocol had 2 steps, using Alexa Fluor 488 rabbit anti-FITC to bind FITC-labeled probes and Alexa Fluor 488 goat anti-rabbit IgG for further enhancement.

Stained cells were analyzed using a FACSCalibur flow cytometer and CellQuest software, version 5.2.1 (Becton Dickinson). For cell lines, live gating was determined by forward

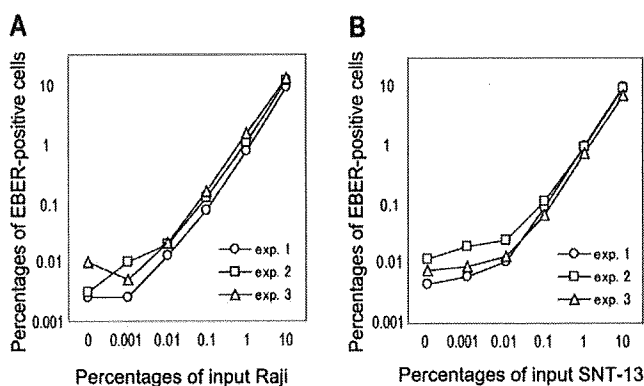


Figure 5. Correlation between the percentage of cells positive for Epstein-Barr virus (EBV)-encoded small RNA (EBER) and input EBV⁺ cells. EBV⁺ and EBV⁻ cells were mixed at various ratios and analyzed by flow cytometric in situ hybridization assay. Each experiment (exp.) was done in triplicate. *A*, B cell lines included Raji (EBV⁺) and BJAB (EBV⁻). *B*, T cell lines included SNT13 (EBV⁺) and Jurkat (EBV⁻).

and side scatter profiles. For PBMCs, lymphocytes were gated by standard forward and side scatter profiles [23]. Up to 50,000 events were acquired for each analysis.

Confocal microscopy. Cells were resuspended in 20 μ L of PermaFluor mounting medium (Thermo) and mounted onto glass slides with coverslips. Samples were examined under an LSM 510 confocal immunofluorescence microscope (Carl Zeiss) [24].

Analyses of EBV DNA. Viral load was examined in the PBMCs of all patients. DNA was extracted from 1×10^6 PBMCs using a QIAamp Blood Kit (Qiagen). Real-time quantitative polymerase chain reaction (PCR) with a fluorogenic probe was performed as described elsewhere [25]. The amount of EBV DNA was calculated as the number of virus copies per microgram of PBMC DNA or per milliliter of whole blood.

To determine which cells harbored EBV, PBMCs were fractionated into CD3⁺, CD19⁺, CD56⁺, TCR $\alpha\beta$ ⁺, and TCR $\gamma\delta$ ⁺ cells using an immunobead method (IMag Cell Separation System; Becton Dickinson) with 97%–99% purity. The fractionated cells were analyzed by real-time quantitative PCR and compared with PBMCs [26]. The clonality of EBV was determined using Southern blotting with a terminal repeat probe, as described elsewhere [27].

Rearrangement of the TCR gene. TCR gene rearrangement was determined by multiplex PCR assays using the T Cell Gene Rearrangement/Clonality assay (InVivoScribe Technologies), which was developed and standardized in a European BIOMED-2 collaborative study [28, 29].

RESULTS

FISH assay to detect EBER. EBV⁺ or EBV⁻ cell lines were fixed, permeabilized, and hybridized with the EBER PNA probe

or negative control PNA probe. After enhancement of fluorescent signals, cells were analyzed by flow cytometry. On the basis of flow cytometry, Raji cells had a significant increase in fluorescence intensity of the EBER PNA probe compared with the negative control PNA probe (Figure 1). Other EBV⁺ B cell lines (Daudi, lymphoblastoid cell line [LCL] 1, and LCL-2) were consistently positive for EBER. In addition to B cell lines, NK cell lines (SNK-1, SNK-6, SNK-10, and KAI3) and EBV⁺ T cell lines (SNT-13 and SNT-16) were also positive for EBER, whereas EBV⁻ B cell (BJAB), NK cell (KHYG-1), and T cell (MOLT-4 and Jurkat) lines were negative for EBER.

Dual staining for surface antigens and EBER. To identify and characterize EBV-infected cells, surface lymphocyte antigens and nuclear EBER must be detected simultaneously. To this end, we first stained surface antigens with PE- or PC5-labeled monoclonal antibodies and then fixed and hybridized the cells with the EBER PNA probe. After enhancement of fluorescence intensity with Alexa Fluor 488 antibodies, both Alexa Fluor 488-labeled EBER and PE- or PC5-labeled surface antigens were detected by flow cytometry. As shown in Figure 2, the EBV⁺ B cell line, Raji, was positive for Alexa Fluor 488-labeled EBER, PE-labeled CD19, and PC5-labeled HLA-DR, but negative for CD2, CD3, CD16, and CD56. In contrast, the EBV⁺ NK cell line, SNK-6, was positive for EBER, CD2, CD56, and HLA-DR, but negative for CD3 and CD19. The EBV⁺ T cell line, SNT-13, was positive for EBER, CD2, and CD3, but negative for CD16, CD19, CD56, and HLA-DR. The EBV⁻ cell line BJAB was negative for EBER, but surface CD19 and HLA-DR antigens were detected (Figure 2).

The dual staining for surface antigens and EBER was further confirmed by confocal microscopy (Figure 3). PE-labeled CD19 and PC5-labeled HLA-DR were present on the surface of both Raji and BJAB cells, whereas Alexa Fluor 488-labeled EBER was specifically detected in the nucleus of Raji cells but not BJAB cells. In contrast, CD3 and CD2 were not present on the surface of Raji cells but were detected on the surface of the EBV⁺ T cell line, SNT-13.

Sensitivity of the FISH assay in identifying EBV⁺ cells. To determine the lower detection limit of the FISH assay for EBV⁺ cells, we mixed EBV⁺ Raji and EBV⁻ BJAB cells in various ratios and analyzed them using the FISH assay (Figure 4). When 10% of Raji cells were mixed with 90% of BJAB cells, 8.9% of CD19⁺EBER⁺ cells could be separated from CD19⁺EBER⁻ cells using the FISH assay. Consistently, as the Raji/BJAB ratio decreased, the percentage of CD19⁺EBER⁺ cells also decreased. EBER⁺ cells could be quantified down to a ratio of 1:10,000 (Raji, 0.01%, CD19⁺EBER⁺ cells, 0.013%), although the population of CD19⁺EBER⁺ cells was not so clear at this ratio. When 0.001% of Raji cells were mixed with BJAB cells, the percentage of CD19⁺EBER⁺ cells was almost equal to 100% of

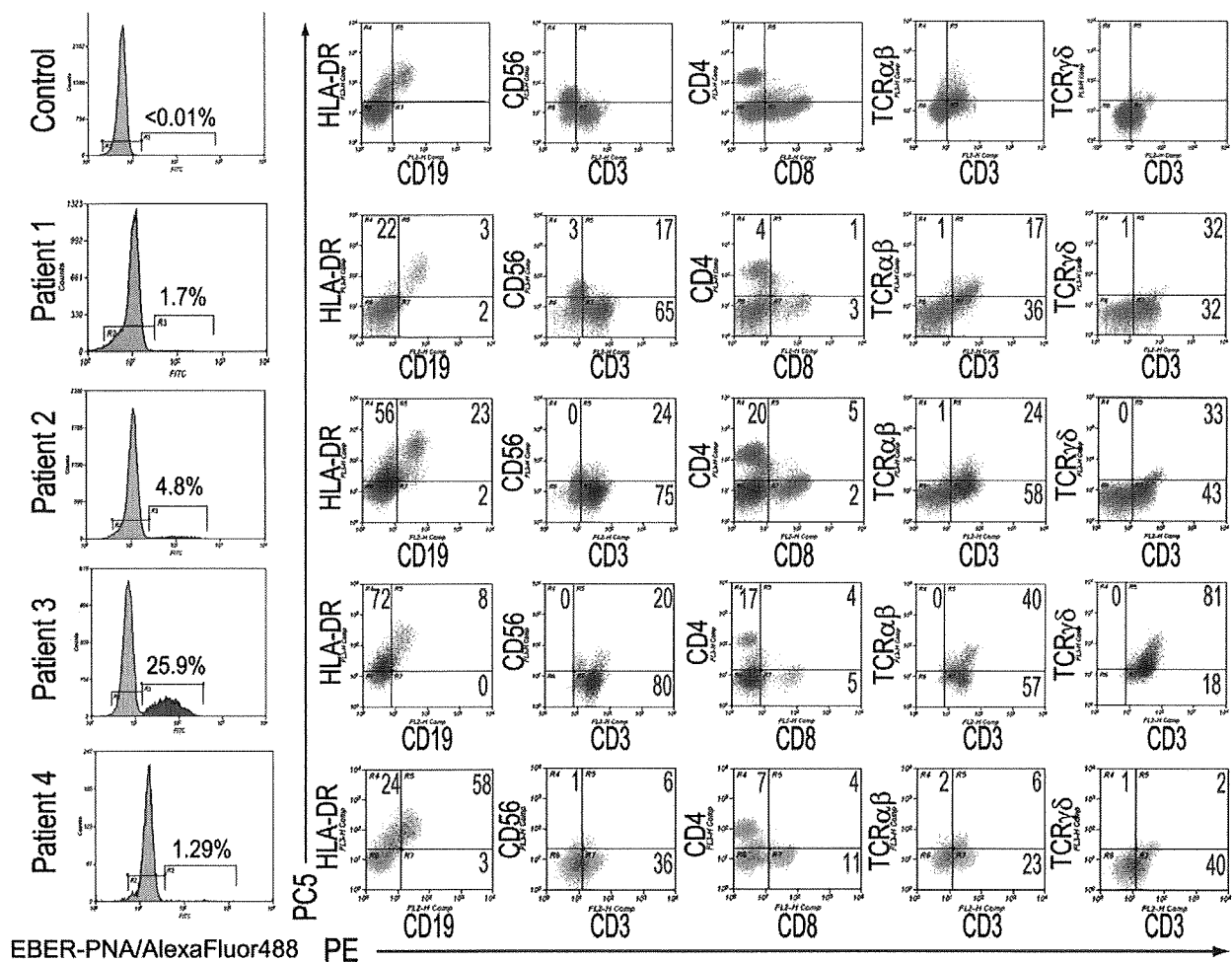


Figure 6. Quantification and identification of Epstein-Barr virus (EBV)-infected lymphocytes in patients with EBV-related lymphoproliferative diseases by flow cytometric in situ hybridization assay. Peripheral blood mononuclear cells were stained with phycoerythrin (PE)-labeled or PE-cyanin 5 (PC5)-labeled monoclonal antibodies and then fixed, permeabilized, and hybridized with the EBV-encoded small RNA (EBER) peptide nucleic acid (PNA) probe. After enhancement of fluorescent signals, the cells were analyzed by flow cytometry. Numbers in histograms represent percentages of EBER⁺ lymphocytes in the total lymphocyte population. EBER⁺ lymphocytes (red) and EBER⁻ lymphocytes (gray) were gated and plotted on quadrants as PE-labeled and PC5-labeled surface antigens. Numbers in quadrants indicate percentages of EBER⁺ cells for each surface immunophenotype. A healthy EBV-seropositive donor served as the control; patients 1–3 had hydroa vacciniforme-like EBV-associated T lymphoproliferative disease, and patient 4 had posttransplantation B cell lymphoproliferative disease. FITC, fluorescein isothiocyanate; TCR, T cell receptor.

BJAB cells (0.003% vs 0.003%), suggesting that the FISH assay was not quantitative at these ratios.

To confirm the accuracy and reproducibility of the FISH assay, we performed the mixing experiments (Raji, EBV⁺ B cell line; BJAB, EBV⁻ B cell line) 2 more times and additional mixing experiments (SNT13, EBV⁺ T cell line; Jurkat, EBV⁻ T cell line) in triplicate. The resulting correlations between the percentage of EBER⁺ cells observed by FISH and the percentage of actual input EBV⁺ cells are shown in Figure 5. These data show a clear correlation at 0.1%–10%, indicating that the assay was able to detect $\geq 0.1\%$ of the EBV⁺ cells accurately and reproducibly.

Application of the FISH assay to human PBMCs. PBMCs were obtained from 5 healthy volunteer donors and analyzed

using the FISH assay. All donors were seropositive for EBV, but EBV DNA was not detected in their PBMCs by real-time PCR. Using the FISH assay, EBER⁺ cells were not detected in any of the donors, whereas the positive control PNA probe directed against glyceraldehyde 3-phosphate dehydrogenase was positive for all PBMCs (data not shown). Dual staining with antibodies to surface antigens and PNA probes showed that most lymphocyte markers were successfully detected and that distinct lymphocyte subsets could be separated, although some surface antigen intensities were not sufficient to separate certain populations (eg, CD56 and TCR $\alpha\beta$). A representative result is shown in Figure 6 (control).

Next, we applied the FISH assay to 3 patients with hydroa vacciniforme-like lymphoproliferative disease. These patients

Table 1. Clinical and Virologic Characteristics of Patients with Epstein-Barr Virus (EBV)-Associated Lymphoproliferative Diseases

Patient	Sex	Age, years	Age at onset, years	Diagnosis	EBV clonality	TCR gene rearrangement	EBV DNA, copies/ μ g DNA					EBV DNA, copies/mL whole blood	
							PBMCs	CD3 ⁺	TCR $\alpha\beta$ ⁺	TCR $\gamma\delta$ ⁺	CD19 ⁺		CD3 ⁻ CD56 ⁺
1	M	16	5	Hydroa vacciniforme	Monoclonal	V γ 1f,V γ 10/J γ ,V δ /J δ	6100	16,380	8310	101,210	ND	860	11,850
2	M	11	5	Hydroa vacciniforme	Monoclonal	V γ 1f,V γ 10/J γ ,V δ /J δ	10,040	13,230	210	87,420	ND	240	ND
3	M	6	3	Hydroa vacciniforme	Monoclonal	V δ /J δ	41,760	46,730	6400	190,100	9090	6400	ND
4	M	6	6	PTLD	ND	ND	22,020	920	ND	ND	91,990	7290	47,660

NOTE. ND, not done; PBMCs, peripheral blood mononuclear cells; PTLD, posttransplantation lymphoproliferative disease; TCR, T cell receptor.

had no symptoms aside from photosensitivity and papulovesicular eruptions on their faces or arms. Skin biopsies were performed in patients 1 and 3. Small lymphoid cells without marked atypia infiltrated both the dermis and epidermis and were positive for EBV. These findings were compatible with hydroa vacciniforme-like lymphoproliferative disease, according to the World Health Organization classification [6]. The infiltrating cells were CD3⁺ but CD56⁻, indicating that they were T cells; further immunophenotyping for TCR $\alpha\beta$ and TCR $\gamma\delta$ was not performed. Extremely high amounts of EBV DNA with monoclonality were detected in the 3 patients' peripheral blood (Table 1). The clonality of the T cells was confirmed based on TCR gene rearrangement. Using the FISH assay, EBV⁺ lymphocytes were detected in their PBMCs, with a frequency of 1.7% in patient 1, 4.8% in patient 2, and 25.9% in patient 3 (Figure 6). We repeated the FISH assay for patients 2 and 3 and obtained similar percentages of EBV⁺ cells (patient 2, 5.0%; patient 3, 20.7%). EBV⁺ lymphocytes were gated and plotted by PE-labeled surface antigens and PC5-labeled surface antigens. Most EBV⁺ lymphocytes were CD3⁺CD4⁻CD8⁻TCR $\gamma\delta$ ⁺ T cells in the 3 patients examined. HLA-DR was expressed in EBV⁺ lymphocytes from patients 2 and 3. To confirm these results, we applied an immunobead method to sort PBMCs into CD3⁺, TCR $\alpha\beta$ ⁺, TCR $\gamma\delta$ ⁺, CD19⁺, and CD3⁻CD56⁺ fractions and used quantitative real-time PCR to quantify EBV DNA in each fraction. The quantity of EBV DNA was high in the CD3⁺ and TCR $\gamma\delta$ ⁺ fractions but not in the CD19⁺, CD3⁻CD56⁺, or TCR $\alpha\beta$ ⁺ fractions (Table 1). For comparison, PBMCs from a patient with posttransplantation B cell lymphoproliferative disease were analyzed by both the FISH assay (Figure 6) and immunobead sorting, followed by EBV DNA quantification (Table 1). Both assays indicated that B cells in the peripheral blood of the patient were EBV⁺, confirming the reliability of the FISH assay.

DISCUSSION

In this study, we established a novel FISH assay to directly quantify and simultaneously characterize EBV-infected lymphocytes using a commercially available EBV PNA probe. The probe is currently used to detect EBV-infected cells in formalin-fixed, paraffin-embedded tissue specimens. Just et al [16] also used this probe in a FISH assay. Crouch et al [30] used oli-

gonucleotide probes directed against EBV in a FISH assay and succeeded in simultaneously detecting both EBV and surface antigens. However, both of these studies used FISH assays only with cell lines, and subsequent application to human PBMCs has not been reported. We preliminarily tested the EBV PNA probe with clinical specimens, but the fluorescence intensity of the probe was not sufficient to separate EBV⁺ peripheral blood cells from EBV⁻ cells (data not shown). By enhancing fluorescence and photostability and modifying the fixation and hybridization steps, we successfully stained both EBV and surface antigens, not only in cell lines but also in human PBMCs. The order of immunophenotyping and ISH is important. We tried the reverse method (ISH preceded by surface immunophenotyping), but no surface antigens were detected by the monoclonal antibodies after ISH (data not shown).

This is a direct method to quantify EBV-infected cells and simultaneously characterize the infected cell phenotype, which helps not only to diagnose EBV-associated diseases but also to select monoclonal antibody-based therapy, such as anti-CD20 (rituximab) or anti-CD52 (Campath-1). We stained only surface lymphocyte markers in this study, but additional surface or intracellular molecules, such as cell adhesion markers, cytotoxic granules, or cytokines, will enable us to characterize and examine the function of EBV-infected lymphocytes. Furthermore, this method can be applied not only to peripheral blood but also to bone marrow and other body fluids, such as ascites, pleural effusions, and cerebrospinal fluid. In addition, FISH can be used for flow cytometric sorting of EBV⁺ cells, which will further expand the ability to isolate and extensively study EBV-infected lymphocytes.

As a noninvasive method to diagnose and monitor EBV-associated lymphoproliferative diseases, measuring viral load in the peripheral blood is a necessary clinical tool. Quantitative PCR assays, such as real-time PCR, are the easiest and most reliable way to measure EBV load and are widely used for diagnosing and managing EBV-associated lymphoproliferative diseases, such as posttransplantation lymphoproliferative disease [7, 31–33]. The FISH assay has some disadvantages compared with quantitative PCR. First, the FISH assay has a lower sensitivity, although it can detect $\geq 0.1\%$ of EBV-infected cells. Second, this assay cannot be applied to EBV-associated diseases

in which EBV-infected cells do not migrate into the peripheral blood, such as nasopharyngeal carcinoma or Hodgkin lymphoma [7, 34, 35]. Another unresolved problem with this assay is that after hybridization, the fluorescent signals of some surface antigens and antibodies were weak and cell separation was incomplete (eg, CD56 and TCR $\alpha\beta$ in Figure 6). We have not clarified this phenomenon completely, but we believe that antigen-antibody complexes were degraded or detached under the harsh hybridization conditions. The extent of this decrease in fluorescent signals differed among antibodies. We screened several monoclonal antibodies with different fluorochromes from different manufacturers for each surface antigen and then selected the best antibodies, as listed in Methods. Thus, selecting the appropriate antibody is important when performing the FISH assay. This problem may be overcome by using better antibodies, cross-linking antibodies or biotin-avidin enhancement, or modifying the fixation or hybridization steps, but the combination of antibodies and the hybridization conditions used in this study are sufficient to separate B, T, and NK cells from other populations.

Hydroa vacciniforme-like lymphoproliferative disease is an EBV⁺ cutaneous malignancy associated with photosensitivity [6]. Although this condition is rare, it affects children and adolescents from Asia and Latin America [36–39]. It is characterized by a papulovesicular eruption that generally proceeds to ulceration and scarring. In some cases, systemic symptoms may be present, including fever, wasting, lymphadenopathy, and hepatosplenomegaly. In hydroa vacciniforme-like eruption, T cells with cytotoxic molecules often infiltrate the superficial dermis and subcutaneous tissues [39]. Most persons with this condition have clonal rearrangement of the TCR genes. EBV in these patients is also monoclonal, as shown terminal repeat analysis. These results indicate that clonal expansion of EBV-infected T cells causes the disease. However, the reported phenotypes of these T cells are variable, and both CD4⁺ and CD8⁺ T cell subsets have been reported [37, 40]. Most studies lack direct confirmation of these cell populations by double-staining with EBER and surface antigens.

In 3 patients with hydroa vacciniforme-like lymphoproliferative disease, we demonstrated that 1.7%–25.9% of peripheral lymphocytes were EBER⁺ and that these lymphocytes were primarily CD3⁺CD4⁻CD8⁻TCR $\gamma\delta$ ⁺ T cells. This is the first study to determine the precise phenotype of EBV-infected lymphocytes in hydroa vacciniforme-like lymphoproliferative disease. $\gamma\delta$ T cells are the major T cell population in the epithelium of the skin and mucosa. They secrete various cytokines and have cytolytic properties [41]. It is possible that EBV-infected $\gamma\delta$ T cells play a central role in the formation of hydroa vacciniforme-like eruptions. The 3 patients examined in this study had no symptoms other than eruptions for several years (3–11 years), although they had a high percentage of clonal, EBV-

infected lymphocytes in their peripheral blood. The prognosis of hydroa vacciniforme-like lymphoproliferative disease has been reported to be variable, and some cases do not progress for up to 10–15 years or seem to spontaneously enter remission [39, 42]. The 3 patients in our study may be exceptional and may not be representative of this patient population. Further investigation with a larger number of patients is needed to conclude that $\gamma\delta$ T cells are the primary EBV-infected cells in hydroa vacciniforme-like lymphoproliferative disease.

Hydroa vacciniforme-like eruption is also seen in severe chronic active EBV infection, which is caused by the clonal expansion of EBV-infected T or NK cells and seen mainly in East Asia [42–45]. These 2 conditions overlap, but their definitions are unclear [6, 46]. Because the 3 patients in the present study had only skin-restricted symptoms, they did not fulfil the classic criteria for chronic active EBV infection [47]. However, both severe chronic active EBV infection and hydroa vacciniforme-like lymphoproliferative disease develop in children and young adults from East Asia and may be caused by the clonal expansion of EBV-infected T or NK cells. To define and differentiate these diseases, additional data on EBV-associated lymphoproliferative diseases are needed. The FISH assay described in this study is a noninvasive, direct, and relatively convenient method to identify and characterize EBV-infected lymphocytes. With this novel method, we hope to further clarify the pathogenesis of EBV-associated lymphoproliferative diseases, including chronic active EBV infection, and to classify each disease more accurately.

Acknowledgments

We thank Tatsuya Tsurumi (Aichi Cancer Center) for the Raji and Daudi cell lines, Akihiro Tomita (Nagoya University Graduate School of Medicine) for the MOLT-4 and Jurkat cell lines, and Norio Shimizu (Tokyo Medical and Dental University) and Ayako Demachi-Okamura (Aichi Cancer Center) for the SNK-1, -6, and -10 and the SNT-13 and -16 cell lines. KAI3 and KHYG-1 were obtained from the Japanese Collection of Research Bioresources. We also thank Tom Just (Dako) for providing valuable comments regarding the FISH assay.

References

1. Straus SE, Cohen JL, Tosato G, Meier J. NIH conference. Epstein-Barr virus infections: biology, pathogenesis, and management. *Ann Intern Med* 1993; 118:45–58.
2. Cohen JL. Epstein-Barr virus infection. *N Engl J Med* 2000; 343:481–92.
3. Williams H, Crawford DH. Epstein-Barr virus: the impact of scientific advances on clinical practice. *Blood* 2006; 107:862–9.
4. Rickinson AB, Kieff E. Epstein-Barr virus and its replication. In: Knipe DM, Howly PM, eds. *Virology*. 5th ed. Vol. 2. Philadelphia: Wolters Kluwer/Lippincott Williams & Wilkins, 2006:2603–54.
5. Rickinson AB, Kieff E. Epstein-Barr virus. In: Knipe DM, Howly PM, eds. *Virology*. 5th ed. Vol. 2. Philadelphia: Wolters Kluwer/Lippincott Williams & Wilkins, 2006:2655–700.
6. Quintanilla-Martinez L, Kimura H, Jaffe ES. EBV⁺ T-cell lymphoma of childhood. In: Swerdlow SH, Campo E, Harris NL, et al, eds. *WHO*

- classification of tumours of haematopoietic and lymphoid tissues. 4th ed. Lyon: WHO Press, 2008:278–80.
7. Kimura H, Ito Y, Suzuki R, Nishiyama Y. Measuring Epstein-Barr virus (EBV) load: the significance and application for each EBV-associated disease. *Rev Med Virol* 2008; 18:305–19.
 8. Randhawa PS, Jaffe R, Demetris AJ, et al. Expression of Epstein-Barr virus-encoded small RNA (by the EBER-1 gene) in liver specimens from transplant recipients with post-transplantation lymphoproliferative disease. *N Engl J Med* 1992; 327:1710–4.
 9. Middeldorp JM, Brink AA, van den Brule AJ, Meijer CJ. Pathogenic roles for Epstein-Barr virus (EBV) gene products in EBV-associated proliferative disorders. *Crit Rev Oncol Hematol* 2003; 45:1–36.
 10. Nielsen PE, Egholm M, Berg RH, Buchardt O. Sequence-selective recognition of DNA by strand displacement with a thymine-substituted polyamide. *Science* 1991; 254:1497–500.
 11. Egholm M, Buchardt O, Christensen L, et al. PNA hybridizes to complementary oligonucleotides obeying the Watson-Crick hydrogen-bonding rules. *Nature* 1993; 365:566–8.
 12. Demidov VV, Potaman VN, Frank-Kamenetskii MD, et al. Stability of peptide nucleic acids in human serum and cellular extracts. *Biochem Pharmacol* 1994; 48:1310–3.
 13. Lansdorp PM, Verwoerd NP, van de Rijke FM, et al. Heterogeneity in telomere length of human chromosomes. *Hum Mol Genet* 1996; 5: 685–91.
 14. Zijlmans JM, Martens UM, Poon SS, et al. Telomeres in the mouse have large inter-chromosomal variations in the number of T2AG3 repeats. *Proc Natl Acad Sci USA* 1997; 94:7423–8.
 15. Lansdorp PM. Telomeres, stem cells, and hematology. *Blood* 2008; 111: 1759–66.
 16. Just T, Burgwald H, Broe MK. Flow cytometric detection of EBV (EBER snRNA) using peptide nucleic acid probes. *J Virol Methods* 1998; 73: 163–74.
 17. Iwatsuki K, Xu Z, Takata M, et al. The association of latent Epstein-Barr virus infection with hydroa vacciniforme. *Br J Dermatol* 1999; 140:715–21.
 18. Nava VE, Jaffe ES. The pathology of NK-cell lymphomas and leukemias. *Adv Anat Pathol* 2005; 12:27–34.
 19. Zhang Y, Nagata H, Ikeuchi T, et al. Common cytological and cytogenetic features of Epstein-Barr virus (EBV)-positive natural killer (NK) cells and cell lines derived from patients with nasal T/NK-cell lymphomas, chronic active EBV infection and hydroa vacciniforme-like eruptions. *Br J Haematol* 2003; 121:805–14.
 20. Tsuge I, Morishima T, Morita M, Kimura H, Kuzushima K, Matsuoka H. Characterization of Epstein-Barr virus (EBV)-infected natural killer (NK) cell proliferation in patients with severe mosquito allergy: establishment of an IL-2-dependent NK-like cell line. *Clin Exp Immunol* 1999; 115:385–92.
 21. Sahai Srivastava BI, Minowada J. Terminal deoxynucleotidyl transferase activity in a cell line (molt-4) derived from the peripheral blood of a patient with acute lymphoblastic leukemia. *Biochem Biophys Res Commun* 1973; 51:529–35.
 22. Yagita M, Huang CL, Umehara H, et al. A novel natural killer cell line (KHYG-1) from a patient with aggressive natural killer cell leukemia carrying a p53 point mutation. *Leukemia* 2000; 14:922–30.
 23. Kuzushima K, Hoshino Y, Fujii K, et al. Rapid determination of Epstein-Barr virus-specific CD8⁺ T-cell frequencies by flow cytometry. *Blood* 1999; 94:3094–100.
 24. Yamauchi Y, Kiriya K, Kubota N, Kimura H, Usukura J, Nishiyama Y. The UL14 tegument protein of herpes simplex virus type 1 is required for efficient nuclear transport of the alpha transactivating factor VP16 and viral capsids. *J Virol* 2008; 82:1094–106.
 25. Kimura H, Morita M, Yabuta Y, et al. Quantitative analysis of Epstein-Barr virus load by using a real-time PCR assay. *J Clin Microbiol* 1999; 37:132–6.
 26. Kimura H, Hoshino Y, Hara S, et al. Differences between T cell-type and natural killer cell-type chronic active Epstein-Barr virus infection. *J Infect Dis* 2005; 191:531–9.
 27. Kimura H, Hoshino Y, Kanegane H, et al. Clinical and virologic characteristics of chronic active Epstein-Barr virus infection. *Blood* 2001; 98:280–6.
 28. van Dongen JJ, Langerak AW, Bruggemann M, et al. Design and standardization of PCR primers and protocols for detection of clonal immunoglobulin and T-cell receptor gene recombinations in suspect lymphoproliferations: report of the BIOMED-2 Concerted Action BMH4-CT98–3936. *Leukemia* 2003; 17:2257–317.
 29. Sandberg Y, van Gastel-Mol EJ, Verhaaf B, Lam KH, van Dongen JJ, Langerak AW. BIOMED-2 multiplex immunoglobulin/T-cell receptor polymerase chain reaction protocols can reliably replace Southern blot analysis in routine clonality diagnostics. *J Mol Diagn* 2005; 7:495–503.
 30. Crouch J, Leitenberg D, Smith BR, Howe JG. Epstein-Barr virus suspension cell assay using in situ hybridization and flow cytometry. *Cytometry* 1997; 29:50–7.
 31. Rooney CM, Loftin SK, Holladay MS, Brenner MK, Krance RA, Heslop HE. Early identification of Epstein-Barr virus-associated post-transplantation lymphoproliferative disease. *Br J Haematol* 1995; 89:98–103.
 32. Rowe DT, Webber S, Schauer EM, Reyes J, Green M. Epstein-Barr virus load monitoring: its role in the prevention and management of post-transplant lymphoproliferative disease. *Transpl Infect Dis* 2001; 3:79–87.
 33. Niesters HG. Molecular and diagnostic clinical virology in real time. *Clin Microbiol Infect* 2004; 10:5–11.
 34. Ambinder RF, Lin L. Mononucleosis in the laboratory. *J Infect Dis* 2005; 192:1503–4.
 35. Chan KC, Zhang J, Chan AT, et al. Molecular characterization of circulating EBV DNA in the plasma of nasopharyngeal carcinoma and lymphoma patients. *Cancer Res* 2003; 63:2028–32.
 36. Barrionuevo C, Anderson VM, Zevallos-Giampietri E, et al. Hydroa-like cutaneous T-cell lymphoma: a clinicopathologic and molecular genetic study of 16 pediatric cases from Peru. *Appl Immunohistochem Mol Morphol* 2002; 10:7–14.
 37. Chen HH, Hsiao CH, Chiu HC. Hydroa vacciniforme-like primary cutaneous CD8-positive T-cell lymphoma. *Br J Dermatol* 2002; 147: 587–91.
 38. Cho KH, Lee SH, Kim CW, et al. Epstein-Barr virus-associated lymphoproliferative lesions presenting as a hydroa vacciniforme-like eruption: an analysis of six cases. *Br J Dermatol* 2004; 151:372–80.
 39. Iwatsuki K, Satoh M, Yamamoto T, et al. Pathogenic link between hydroa vacciniforme and Epstein-Barr virus-associated hematologic disorders. *Arch Dermatol* 2006; 142:587–95.
 40. Doeden K, Molina-Kirsch H, Perez E, Warnke R, Sundram U. Hydroa-like lymphoma with CD56 expression. *J Cutan Pathol* 2008; 35:488–94.
 41. Kaufmann SH. gamma/delta and other unconventional T lymphocytes: what do they see and what do they do? *Proc Natl Acad Sci U S A* 1996; 93:2272–9.
 42. Nitta Y, Iwatsuki K, Kimura H, et al. Fatal natural killer cell lymphoma arising in a patient with a crop of Epstein-Barr virus-associated disorders. *Eur J Dermatol* 2005; 15:503–6.
 43. Kanegane H, Nomura K, Miyawaki T, Tosato G. Biological aspects of Epstein-Barr virus (EBV)-infected lymphocytes in chronic active EBV infection and associated malignancies. *Crit Rev Oncol Hematol* 2002; 44:239–49.
 44. Kimura H, Morishima T, Kanegane H, et al. Prognostic factors for chronic active Epstein-Barr virus infection. *J Infect Dis* 2003; 187:527–33.
 45. Katagiri Y, Mitsuhashi Y, Kondo S, Kanazawa C, Iwatsuki K, Tsunoda T. Hydroa vacciniforme-like eruptions in a patient with chronic active EB virus infection. *J Dermatol* 2003; 30:400–4.
 46. Ohshima K, Kimura H, Yoshino T, et al. Proposed categorization of pathological states of EBV-associated T/natural killer-cell lymphoproliferative disorder (LPD) in children and young adults: overlap with chronic active EBV infection and infantile fulminant EBV T-LPD. *Pathol Int* 2008; 58:209–17.
 47. Straus SE. The chronic mononucleosis syndrome. *J Infect Dis* 1988; 157:405–12.

T Cell–Mediated Control of Epstein-Barr Virus Infection in Humanized Mice

Misako Yajima,¹ Ken-Ichi Imadome,¹ Atsuko Nakagawa,² Satoru Watanabe,³ Kazuo Terashima,⁴ Hiroyuki Nakamura,¹ Mamoru Ito,⁵ Norio Shimizu,³ Naoki Yamamoto,⁵ and Shigeyoshi Fujiwara¹

¹Department of Infectious Diseases, National Research Institute for Child Health and Development, and ²Pathology Laboratory, Department of Clinical Laboratory Medicine, National Center for Child Health and Development, Setagaya-ku, ³Department of Virology, Division of Medical Science, Medical Research Institute, and ⁴Department of Pathology, Faculty of Medicine, Tokyo Medical and Dental University, Bunkyo-ku, and ⁵AIDS Research Center, National Institute of Infectious Diseases, Shinjuku-ku, Tokyo, and ⁶Central Institute for Experimental Animals, Kawasaki, Kanagawa, Japan

Humanized NOD/Shi-*scid*/interleukin-2R γ ^{null} (NOG) mice with full T cell development had significantly longer life span after Epstein-Barr virus (EBV) infection, compared with those with minimal T cell development. Removing CD3⁺ or CD8⁺ T cells from EBV-infected humanized mice by administration of anti-CD3 or anti-CD8 antibodies reduced their life span. CD8⁺ T cells obtained from EBV-infected mice suppressed the outgrowth of autologous B cells isolated from uninfected mice and inoculated with EBV *in vitro*. These results indicate that humanized NOG mice are capable of T cell–mediated control of EBV infection and imply their usefulness as a tool to evaluate immunotherapeutic and prophylactic strategies for EBV infection.

Epstein-Barr virus (EBV) is a ubiquitous B-lymphotropic herpesvirus, and >90% of the adult population in the world is latently infected with the virus [1]. Although EBV is an important etiological factor in various malignancies, including endemic Burkitt lymphoma, Hodgkin lymphoma, and nasopharyngeal carcinoma, most EBV infection is asymptomatic

and persists for life without any signs or symptoms. EBV has a unique ability to transform human B lymphocytes *in vitro* and to establish immortalized lymphoblastoid cell lines [2]. EBV-transformed lymphoblastoid cell lines express 9 viral proteins, most of which serve as efficient targets of EBV-specific T cell responses [2]. In immunologically competent hosts, therefore, EBV-transformed cells are readily removed by EBV-specific cytotoxic T lymphocytes [3], and EBV persistence is restricted to memory B cells, in which the expression of all viral proteins is shut down [4]. In immunocompromised hosts, however, EBV-infected B lymphoblasts can proliferate to cause lymphoproliferative disorder [1]. Thus, EBV persistence in human hosts is based on a fine balance between the host immunosurveillance, especially the function of EBV-specific cytotoxic T lymphocytes, and the replicative potential of EBV and the growth potential of EBV-infected cells.

Recently, we developed a new humanized mouse model of EBV infection, based on the NOD/Shi-*scid*/interleukin-2R γ ^{null} (NOG) mouse strain [5], that can reproduce key aspects of human EBV infection, such as lymphoproliferative disorder, asymptomatic persistent infection, and humoral and T cell–mediated immune responses [6]. In this model, inoculation with high-dose EBV ($\sim 1 \times 10^3$ 50% transformation dose [TD₅₀]) resulted in the development of lymphoproliferative disorder, whereas inoculation with low-dose virus ($\leq 1 \times 10^1$ TD₅₀) tended to cause apparently asymptomatic persistent infection. Enzyme-linked immunosorbent assay and flow cytometry identified CD8⁺ T cells that recognize autologous EBV-transformed lymphoblastoid cells and produce IFN- γ in a human major histocompatibility complex class I–restricted manner [6]. Although immune responses to EBV have been demonstrated in this NOG mouse model and other types of humanized mice [7, 8], whether these immune responses work functionally to control EBV infection has not been clarified. To address this issue, we examined whether T cells in humanized NOG mice have any influence on the survival of EBV-infected mice. We also tested whether CD8⁺ T cells isolated from EBV-infected NOG mice have a capacity to suppress EBV-induced lymphocyte transformation.

Methods. NOG mice were obtained from the Central Institute for Experimental Animals, and cord blood samples were supplied by the Tokyo Cord Blood Bank after obtaining informed consent. Reconstitution of human immune system components was performed as described elsewhere [6, 9, 10]. In brief, CD34⁺ human hematopoietic stem cells (HSCs) were isolated from cord blood with use of the MACS Direct CD34 Progenitor Cell Isolation Kit (Miltenyi Biotec), and 1×10^4 –

Received 14 May 2009; accepted 19 June 2009; electronically published 15 October 2009.
Potential conflicts of interest: none reported.

Financial support: Ministry of Health, Labour and Welfare of Japan (H19-AIDS-003 and H21-AIDS-008) and a grant for the Research on Publicly Essential Drugs and Medical Devices from The Japan Health Sciences Foundation.

Reprints or correspondence: Dr. Shigeyoshi Fujiwara, Dept. of Infectious Diseases, National Research Institute for Child Health and Development, 2-10-1 Okura, Setagaya-ku, Tokyo 157-8535, Japan (shige@nch.go.jp).

The Journal of Infectious Diseases 2009;200:1611–15

© 2009 by the Infectious Diseases Society of America. All rights reserved.
0022-1899/2009/20010-0018\$15.00
DOI: 10.1093/infdis/jin161

1.2×10^5 cells/mouse of HSCs were transplanted in 6–10-week-old female NOG mice via the tail vein. The development of human blood cells in the peripheral blood was monitored by staining with monoclonal antibodies specific to human CD45RA, CD45RO, CD19, CD3, CD4, and CD8. NOG mice in which the human hematoinmune system was recon-

stituted are referred to here as humanized NOG mice. The term “lot” signifies a group of humanized mice derived from a single cord blood donor. Protocols of experiments with NOG mice were approved by the Institutional Animal Care and Use Committee of the National Institute of Infectious Diseases. The use of human materials in this research was approved by the In-

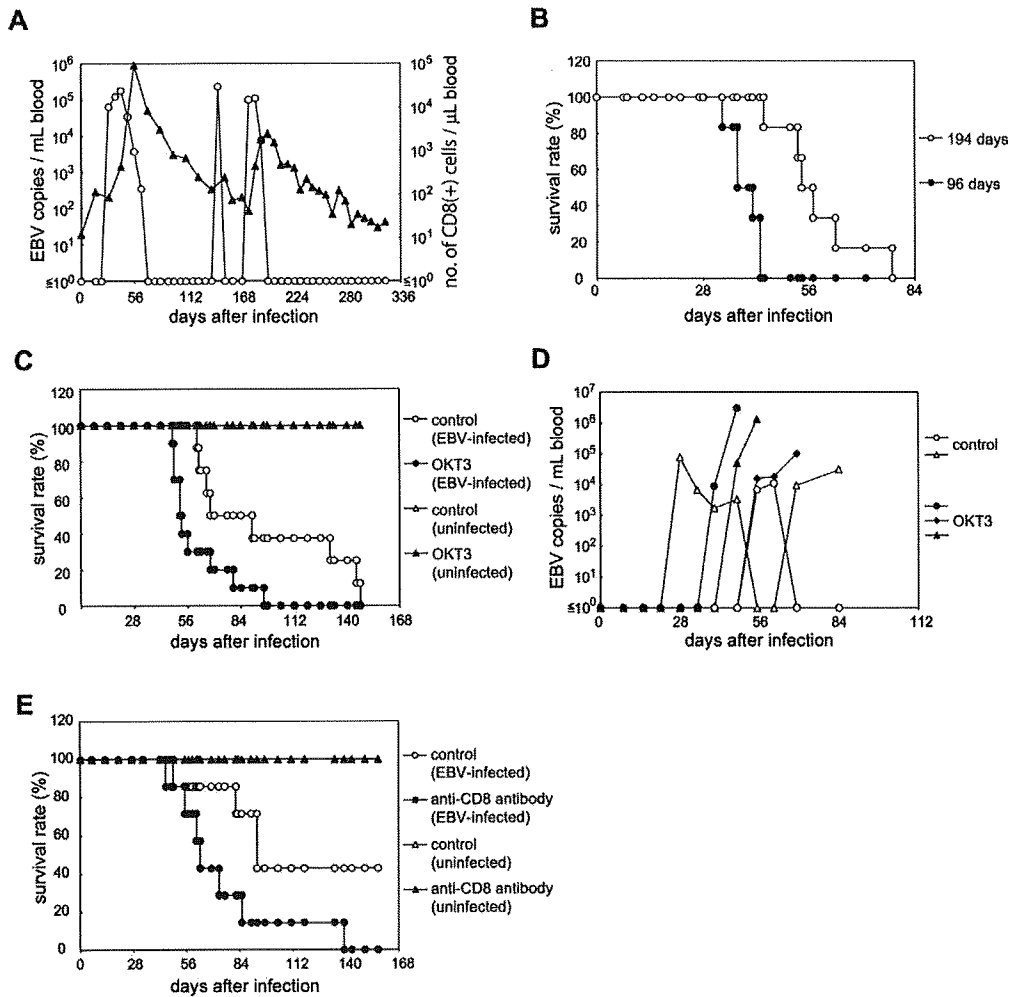


Figure 1. Evidence for T cell-mediated control of Epstein-Barr virus (EBV) infection in humanized NOD/Shi-*scid*/interleukin-2R γ^{null} (NOG) mice. *A*, Associated changes in the number of CD8⁺ T cells and viral DNA level in the peripheral blood of an EBV-infected humanized NOG mouse inoculated with EBV at ten 50% transformation dose (TD_{50}). The levels of EBV DNA (*open circles*) and CD8⁺ T cells (*black triangles*) were monitored periodically. *B*, Survival curves of humanized NOG mice inoculated with EBV at different stages of reconstitution with human lymphocytes. Black circles represent mice inoculated with EBV (1×10^3 TD_{50}) at 96 days after transplantation with hematopoietic stem cells, and open circles represent mice inoculated at 194 days. *C*, Effect of depletion of T cells on the survival of EBV-infected humanized NOG mice. Black circles represent mice given daily intravenous injection with the OKT3 antibody ($2 \mu\text{g}/\text{mouse}/\text{day}$), starting at 21 days after infection, and open circles represent mice not given the antibody. Black triangles represent EBV-uninfected humanized NOG mice given OKT3 antibody, and open triangles represent such mice not given the antibody. *D*, Effect of depletion of T cells on the peripheral blood level of EBV DNA in humanized NOG mice. Black circles, black triangles, and black diamonds represent 3 humanized NOG mice inoculated with EBV (1×10^3 TD_{50}) that were treated with OKT3 as described in *C*, and open circles and open triangles represent such mice not treated with the antibody. Interruption of records indicates the death of a mouse. *E*, Effect of antibody specific to the CD8 molecule (B9.11) on the survival of EBV-infected humanized NOG mice. Black circles represent EBV-infected humanized NOG mice given daily intravenous injection with B9.11 ($2 \mu\text{g}/\text{mouse}/\text{day}$), starting at 21 days after infection, and open circles represent such mice not given the injection. Black triangles represent humanized NOG mice not infected with EBV that were given OKT3 antibody, and open triangles represent such mice not given the antibody.

stitutional Review Boards of the National Research Institute for Child Health and Development, the National Institute of Infectious Diseases, and the Tokyo Cord Blood Bank.

Preparation of EBV inocula and their titration, intravenous inoculation to humanized NOG mice, and quantification of viral DNA were performed as described elsewhere [6]. In brief, virus production from Akata cells was stimulated by treatment with anti-IgG antibody (DAKO), and culture fluid was used as inoculum after filtration through a 0.45- μ m membrane filter. EBV titers in TD_{50} were determined by the Reed-Muench method.

In T cell reduction experiments, humanized NOG mice were inoculated with EBV at a dose of 1×10^2 TD_{50} . Starting at 21 days after inoculation, the Orthoclone OKT3 antibody specific to CD3 (Janssen Pharmaceutical) or the B9.11 antibody specific to CD8 (Beckman-Coulter) was administered intravenously at a dosage of 2 μ g/mouse/day everyday until the end of the experiment. In a typical mouse treated with OKT3, 0.1% of human $CD45^+$ cells were $CD4^+CD8^-$ and 0.8% were $CD4^-CD8^+$ 2 weeks after the initiation of OKT3 administration, whereas in a control mouse, 15.0% of human $CD45^+$ cells were $CD4^+CD8^-$ and 12.5% were $CD4^-CD8^+$. Thus, this antibody was effective in significantly reducing the number of specific target cells. Confirmation of the reduction of $CD8^+$ cells by B9.11 was not possible, because this antibody covered the epitope recognized by antibodies available for flow cytometry. Survival curves of antibody-treated and untreated mice were compared statistically by the log-rank test.

Direct suppression of EBV-induced B cell transformation by $CD8^+$ T cells was assessed by the transformation regression assay based on a previously described method [11, 12]. $CD8^+$ T cells were isolated, as described elsewhere [6], from the spleen of EBV-infected or uninfected humanized NOG mice. Mononuclear cells were isolated from the spleen of uninfected humanized NOG mice and were inoculated with EBV (3×10^3 TD_{50} per 1×10^7 splenocytes). These EBV-infected cells were dispensed into microplates (3×10^4 – 1×10^5 cells/well) and were mixed with $CD8^+$ T cells in the wells of microculture plates at different ratios. Half of the medium was replaced with fresh medium each week, and the outgrowth of lymphoblastoid cell lines was counted 8 weeks after initiation of the culture. Humanized NOG mice in the same lot were used in each experiment to attain common background of human major histocompatibility complex. The number of $CD8^+$ T cells required to achieve regression in 50% of the wells (50% regression dose) was calculated by the Reed-Muench method.

Results. Our previous experiments indicated that EBV-infected humanized NOG mice mount an EBV-specific T cell response that may be involved in immunological control of EBV. A time course of the levels of EBV DNA and $CD8^+$ T

Table 1. Fifty Percent Regression Dose of $CD8^+$ T Cells in Epstein-Barr Virus (EBV)-Infected and Uninfected Mice

Experiment ^a	50% Regression dose	
	EBV-infected mice	Uninfected mice
A1	2.7×10^4	$>9.9 \times 10^4$
B1-1	2.7×10^5	$>1.4 \times 10^6$
B1-2	2.4×10^5	$>8.5 \times 10^5$
B2	1.1×10^5	$>4.2 \times 10^5$
B3 ^b	$>2.3 \times 10^5$	$>3.0 \times 10^5$
C1 ^b	$>3.9 \times 10^5$	$>3.2 \times 10^5$
C2	2.0×10^4	$>1.7 \times 10^5$

^a Alphabetical letters signify the lot of a mouse, and the number immediately after the letter indicates an individual mouse. Numbers after a hyphen identify individual experiments.

^b No significant regression was seen in these experiments.

cells in the peripheral blood of a representative EBV-infected mouse (Figure 1A) suggested that these parameters change in an associated manner; there was a tendency for $CD8^+$ T cells to increase after surges in the EBV DNA level and to gradually decrease as the EBV DNA level decreased, suggesting that these $CD8^+$ T cells have some role in the control of EBV DNA level.

To examine the protective role of T cells more precisely, we next tested whether the development of T cells has any influence on the mice's resistance to EBV infection. After transplantation with human HSCs, B cells develop first, \sim 3 months after transplantation, and T cells differentiate later, \sim 6 months after transplantation [10]. We divided 12 humanized NOG mice in a lot into 2 groups; 6 mice were inoculated with EBV (1×10^3 TD_{50}) at 96 days after transplantation with HSCs, and the remaining 6 were inoculated at 194 days. Mice were examined daily, and those exhibiting signs of severe illness, including weight loss, piloerection, and cachexia, were sacrificed for analysis. On autopsy, most of these mice showed the signs of lymphoproliferative disorder, as described elsewhere [6]. Figure 1B shows the survival curve of each group of infected mice, and the log-rank test indicated that the mice inoculated at 6 months after transplantation (ie, with fully developed T cells) had a significantly elongated life span ($P < .001$).

Because the aforementioned results suggested that T lymphocytes reconstituted in humanized NOG mice have some role in the protection against EBV-induced lymphoproliferative disorder, we then examined the effect of the anti-CD3 monoclonal antibody OKT3, which can deplete T cells in vivo [13]. Eighteen humanized NOG mice inoculated with 1×10^2 TD_{50} EBV were divided into 2 groups; 10 mice were given OKT3 beginning at 21 days after inoculation, and the remaining 8 were not given the antibody. Figure 1C shows the survival curve of these mice. The log-rank test indicated that those mice treated with OKT3 antibody had a significantly shorter life span, compared with control mice ($P < .01$). Similar OKT3 treatment